

Energy & Environmental Science

Accepted Manuscript



This is an *Accepted Manuscript*, which has been through the Royal Society of Chemistry peer review process and has been accepted for publication.

Accepted Manuscripts are published online shortly after acceptance, before technical editing, formatting and proof reading. Using this free service, authors can make their results available to the community, in citable form, before we publish the edited article. We will replace this *Accepted Manuscript* with the edited and formatted *Advance Article* as soon as it is available.

You can find more information about *Accepted Manuscripts* in the [Information for Authors](#).

Please note that technical editing may introduce minor changes to the text and/or graphics, which may alter content. The journal's standard [Terms & Conditions](#) and the [Ethical guidelines](#) still apply. In no event shall the Royal Society of Chemistry be held responsible for any errors or omissions in this *Accepted Manuscript* or any consequences arising from the use of any information it contains.



Journal Name

COMMUNICATION

Stable semi-transparent $\text{CH}_3\text{NH}_3\text{PbI}_3$ planar sandwich solar cells

Jun Hyuck Heo^a, Hye Ji Han^a, Minho Lee^a, Myungkwan Song^b, Dong Ho Kim^b, Sang Hyuk Im^{a,*}

Received 00th January 20xx,
Accepted 00th January 20xx

DOI: 10.1039/x0xx00000x

www.rsc.org/

Semi-transparent $\text{CH}_3\text{NH}_3\text{PbI}_3$ (MAPbI_3) planar sandwich solar cells could be fabricated by simply laminating an FTO (F doped tin oxide)/ TiO_2 / MAPbI_3 /wet hole transporting material (HTM) with additives and a PEDOT:PSS (poly(3,4-ethylenedioxythiophene): poly(styrenesulfonic acid))/indium tin oxide (ITO). The best device of FTO/ TiO_2 / MAPbI_3 /P3HT with additives/PEDOT:PSS/ITO planar sandwich structured solar cell exhibited 12.8 % (deviation: 11.7 % \pm 0.74 %) of average power conversion efficiency (η_{avg}) but poor visible transmittance due to strong absorption by P3HT. Whereas, semi-transparent FTO/ TiO_2 / MAPbI_3 /PTAA with additives/PEDOT:PSS/ITO planar sandwich solar cells exhibited 15.8 % (deviation: 14.45 % \pm 0.76 %) of η_{avg} without significant J-V hysteresis with respect to the forward and reverse scan direction. The average visible transmittance (AVT) was controlled from 17.3 % to 6.3 % and its corresponding η_{avg} was changed from 12.55 % to 15.8 %. The unsealed sandwich planar perovskite solar cells exhibited great air and humidity stability over 20 days due to the self-passivated device architecture of sandwich type device.

Solar energy has been considered as a promising candidate compensating the conventional fossil fuels because it is clean, abundant, and sustainable. Therefore, the solar cells have been intensively studied for several decades and to date, the crystalline Si solar cells are widely installed at remote area for power generation. However, the power generation cost of crystalline Si solar cells is still more expensive than the fossil fuels so it is strongly required to develop cost-effective solar cells in order to expand their utilization in our daily life such as building integrated photovoltaics (BIPVs) and mobile power sources.

For this, organic photovoltaics, thin-film solar cells, and sensitized solar cells have been of great interest to meet the satisfaction of

low cost and high device efficiency. Among them, the sensitized solar cells have unique device architecture of electron conductor, sensitizer, and hole conductor so that high efficiency can be achieved by using relatively impure materials because the generated electrons (holes) are immediately injected into electron conductor (hole conductor) thereby reducing the backward recombination.

Recently Kojima *et al.*[1] reported the innovative sensitized solar cells utilizing organic-inorganic hybrid perovskite sensitizers having prominent properties such as strong absorption by direct bandgap,[2] high open circuit voltage (V_{oc}) due to small exciton binding energy,[3] and long diffusion length of charge carriers.[4] Since then, all solid-state mesoscopic,[5] planar,[6] and meso-structured[7] perovskite hybrid solar cells have been developed and the record efficiency reached upto 17.9 % [8] under illumination of 100 mW/cm^2 AM 1.5G.

However, the $\text{CH}_3\text{NH}_3\text{PbI}_3$ (MAPbI_3) or $\text{CH}_3\text{NH}_3\text{PbI}_{3-x}\text{Cl}_x$ perovskite hybrid solar cells comprised to TCO (transparent conducting oxide)/electron conductor/perovskite/hole conductor/metal counter electrode often exhibited significant hysteresis of power conversion efficiency with respect to the forward and backward scan direction[9] and weak stability to humidity[10]. The origin of J-V (current density-voltage) hysteresis with respect to the scan direction and scan rate is still under debate. The J-V hysteresis might be occurred by the capacitance element of perovskite device which might be related with the charge accumulation at traps [6j, 6k, 11] or the dielectric polarization[12] due to the ferroelectric properties. The weak humidity stability of perovskite materials will be associated with the fact that they can be decomposed to MAI and PbI_2 by the humidity. Therefore, it is still challenging to develop sandwich type of semi-transparent planar perovskite hybrid solar cells without J-V hysteresis with respect to the scan direction because the sandwich device architecture analogy to dye sensitized solar cells enables demonstration of semi-transparent cells and better protection from invasion of water vapor owing to the two TCO electrodes.

Eperon *et al.*[13] reported semi-transparent island-morphology- $\text{MAPbI}_{3-x}\text{Cl}_x$ perovskite solar cells with neutral color composed to FTO (F-dope tin oxide)/compact TiO_2 /thickness controlled MAPbI_3 .

^a Functional Crystallization Center (FCC), Department of Chemical Engineering, Kyung Hee University, 1732 Deogyong-daero, Giheung-gu, Yongin-si, Gyeonggi-do 446-701, Republic of Korea, E-mail: imrom@khu.ac.kr

^b Advanced Functional Thin Film Department, 797 Changwondaero, Seongsangu, Changwon, Gyeongnam, 642-831, Republic of Korea

Electronic Supplementary Information (ESI) available: [details of any supplementary information available should be included here]. See DOI: 10.1039/x0xx00000x

$x\text{Cl}_x$ islands/Spiro-MeOTAD (2,2',7,7'-tetrakis-(N,N-dip-methoxyphenylamine)-9,9'-spirobifluorene)/Au. Ono *et al.*[14] also reported semi-transparent thin-film-MAPbI_{3-x}Cl_x perovskite solar cells comprised to FTO/compact TiO₂/hybrid deposited MAPbI_{3-x}Cl_x thin-film/Spiro-MeOTAD/Ag but they exhibited significant J-V hysteresis with respect to the scan direction. Roldán-Carmona *et al.*[15] reported semi-transparent planar MAPbI₃ perovskite solar cells consisted of ITO (indium tin oxide)/PEDOT:PSS (poly(3,4-ethylenedioxythiophene):poly(styrenesulfonic acid))/vacuum deposited MAPbI₃/Poly-TPD (Poly[N,N'-bis(4-butylphenyl)-N,N'-bis(phenyl)benzidine])/PCBM ([6,6]-phenyl C₆₁-butyric acid methylester)/Au/LiF. Li *et al.*[16] reported 6.87 % semi-transparent MAPbI₃ solar cells with laminated metal-free carbon nanotube (CNT) network electrode and their efficiency could be improved to 9.9 % by using composite electrode of CNT network and spiro-MeOTAD. Guo *et al.*[17] reported 8.49 % semi-transparent MAPbI_{3-x}Cl_x solar cells with ZnO/Ag nanowire transparent electrode. So far, to our best knowledge, the sandwich type semi-transparent planar perovskite thin-film solar cells using transparent top and bottom electrode like the dye sensitized solar cells have not reported yet, although the sandwich type device architecture has advantage of self-passivation, thereby improving stability. Here we fabricated 15.8 % semi-transparent planar MAPbI₃ perovskite hybrid sandwich solar cells without significant J-V hysteresis with respect to the scan direction (forward scan efficiency = 15.7 %, backward scan efficiency = 15.9 % under illumination of 100 mW/cm² AM 1.5G, delay time = 200 ms).

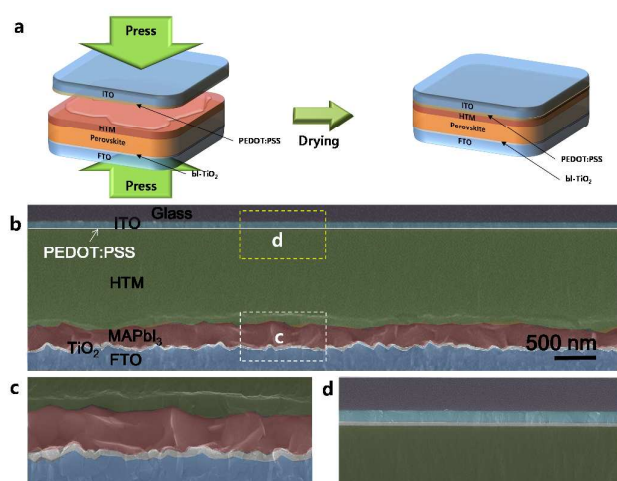


Fig. 1. (a) Schematic illustration for device fabrication and architecture of MAPbI₃ planar sandwich solar cell, (b) representative SEM cross-sectional image of full sandwich cell consisted of FTO/TiO₂/MAPbI₃/HTM/PEDOT:PSS/ITO/Glass, and its magnified image of (c) FTO/TiO₂/MAPbI₃/HTM part and (d) HTM/PEDOT:PSS/ITO/Glass part.

Fig. 1 shows a schematic illustration of device fabrication and representative device architecture of a semi-transparent MAPbI₃ planar sandwich solar cell. In a typical fabrication procedure (see **Fig. 1(a)**), we deposited ~50 nm-thick TiO₂ electron conductor on a cleaned FTO substrate by spraying 20 mM of titanium diisopropoxide bis(acetylacetonate) solution at 450 °C. A pin-hole

free pure MAPbI₃ thin-film was then deposited on the TiO₂/FTO substrate by spin-coating of 40 wt% MAPbI₃ in DMF (N,N-dimethylformamide) solution containing additional 10 vol % of HI solution at 3000 rpm for 200 s and subsequent drying at 100 °C for 2 min under ambient atmosphere. A counter electrode was prepared by spin-coating of a filtered PEDOT:PSS (poly(3,4-ethylenedioxythiophene):poly(styrenesulfonic acid))/methanol (1:2 vol:vol) solution on a cleaned ITO (indium tin oxide) glass substrate at 3000 rpm for 60s and subsequent drying at 150 °C for 20 min. A P3HT (poly-3-hexylthiophene) or PTAA (poly-triarylamine) [18] hole transporting material (HTM)/toluene solution with Li-TFSI (Li-bis(trifluoromethanesulfonyl) imide):ACN (acetonitrile) solution and t-BP (tert-butylpyridine):ACN solution additives (HTM/toluene/Li-TFSI:ACN/t-BP:ACN = 20 mg/1 mL/15 μL (170 mg: 1 mL)/30 μL (1 mL: 1mL) was drop-casted on the MAPbI₃/TiO₂/FTO substrate and the counter electrode of PEDOT:PSS/ITO substrate was covered on the wet HTM/MAPbI₃/TiO₂/FTO substrate. Then the two substrates were pressurized by double clip and subsequently were dried (see **Fig. S1**). **Fig. 1(b)** shows a SEM (scanning electron microscope) cross-sectional image of the semi-transparent MAPbI₃ planar sandwich solar cell comprised to ITO/PEDOT:PSS/HTM with additives/MAPbI₃/TiO₂/FTO. The magnified images were the HTM with additives/MAPbI₃/TiO₂/FTO (**Fig. 1(c)**) and ITO/PEDOT:PSS/HTM with additives (**Fig. 1(d)**) part in the sandwich solar cell. From the SEM cross-sectional image of the best device, the thickness of TiO₂, MAPbI₃, HTM with additives, and PEDOT:PSS layer was ~50 nm, ~300 nm, ~1200 nm, and ~30 nm, respectively.

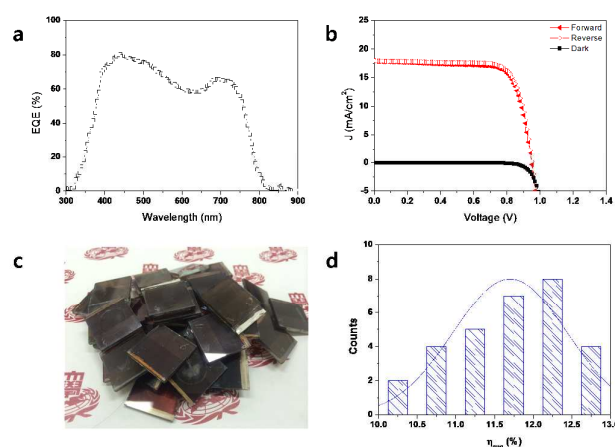


Fig. 2. (a) EQE (external quantum efficiency) spectrum, (b) J-V (current density-voltage) curves (scan rate = 10 mV/200 ms, delay time = 200 ms), (c) photographs, and (d) deviation of average power conversion efficiency (η_{avg}) of FTO/TiO₂/MAPbI₃/P3HT with additives/PEDOT:PSS/ITO planar sandwich solar cell.

Table 1. Summary of photovoltaic properties of FTO/TiO₂/MAPbI₃/P3HT with additives/PEDOT:PSS/ITO planar sandwich solar cell with respect to the scan direction.

Device	Scan direction	V _{oc} (V)	J _{sc} (mA/cm ²)	F.F (%)	η (%)	η _{avg} (%)	Deviation
P3HT	Forward	0.94	18	75	12.7	12.8	11.7±0.74
	Reverse	0.95	18	76	12.9		

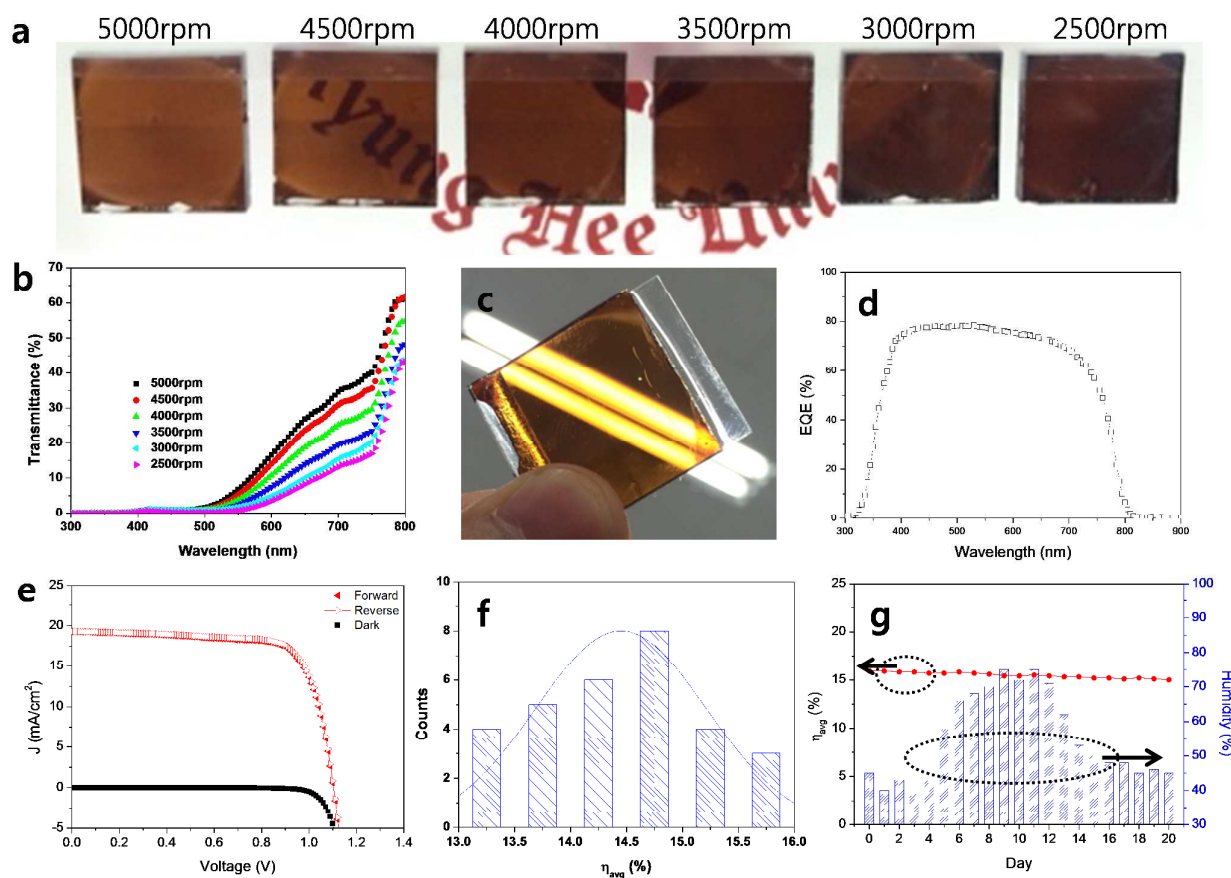


Fig. 3. (a) photographs of FTO/TiO₂/MAPbI₃ films with controlled thickness by spin speed from 5000 rpm to 2500 rpm, (b) their corresponding transmission spectra, (c) photograph of full FTO/TiO₂/MAPbI₃/PTAA with additives/PEDOT:PSS/ITO planar sandwich solar cell (2500 rpm sample), (d) its corresponding EQE spectrum, (e) J-V curves with respect to the forward and the reverse scan direction (scan rate = 10 mV/200 ms, delay time = 200 ms, front illumination to FTO side), (f) deviation of average power conversion efficiency (η_{avg}) of 2500 rpm samples, and (g) device stability of unsealed 2500 rpm sample with storage time.

Fig. 2 shows photovoltaic properties of ITO/PEDOT:PSS/P3HT with Li-TFSI and t-BP additives/MAPbI₃/TiO₂/FTO planar sandwich solar cells. The EQE (external quantum efficiency) spectrum in **Fig. 2(a)** reached upto ~80% and appeared the dimple at ~ 650 nm-wavelength due to the absorption by P3HT HMT possibly due to partial reflection by ITO electrode. The J-V curve of back illumination was shown in **Fig. S2(a)** indicating that the average efficiency is greatly reduced from 12.8 % to 10.0 % by the light absorption of P3HT because the J_{sc} is greatly reduced to 15.1 mA·cm⁻² compared to the front illuminated case (18 mA·cm⁻²). The integrated value of EQE spectrum is ~18 mA·cm⁻², which is lower than that in MAPbI₃ perovskite hybrid solar cells with Au metal reflecting counter electrode[5f], because the ~300 nm-thick MAPbI₃ can absorb ~90% of illuminated light due to the strong absorptivity of MAPbI₃ having direct bandgap.[2] The J-V curves of MAPbI₃ planar sandwich cell in **Fig. 2(b)** exhibited that 0.94 V open circuit voltage (V_{oc}), 18 mA·cm⁻² short circuit current density (J_{sc}), 75% fill factor (F.F), and 12.7 % power conversion efficiency (η) was

obtained under forward scan direction and 0.95 V V_{oc} , 18 mA·cm⁻² J_{sc} , 76% F.F, and 13 % η was done under reverse scan direction, respectively (see the **Table 1**), thereby showing 12.8 % average power conversion efficiency (η_{avg}). The planar perovskite sandwich solar cells with high quality MAPbI₃ did not show significant J-V hysteresis with respect to the scan direction but the apparent transparency of sandwich solar cell in visible region was not good due to the strong absorption of visible light by the thick P3HT HMT with additives (see the 30 samples of MAPbI₃/P3HT with additives planar sandwich solar cells in **Fig. 2(c)**). The deviation of η_{avg} of 30 samples shown in **Fig. 2(d)** indicates that the MAPbI₃ planar sandwich solar cells can be reproducibly fabricated by the simple lamination process.

The transparency of solar cells is very important to find application to the BIPVs. Therefore, we switched the P3HT HMT with absorption in visible region to the transparent PTAA HMT. **Fig. 3(a)** shows the photographs of FTO/TiO₂/MAPbI₃ with controlled thickness by the spin-speed. The transmittance of perovskite film at

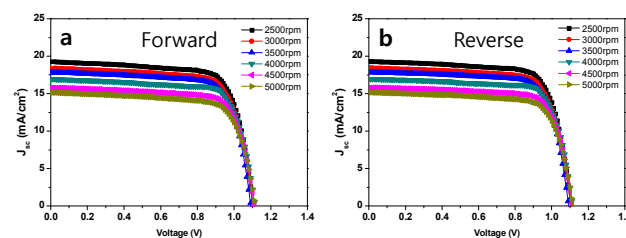
Table 2. Summary of photovoltaic properties of FTO/TiO₂/MAPbI₃ with controlled thickness by spin speed (rpm)/PTAA with additives/PEDOT:PSS/ITO planar sandwich solar cell with respect to the scan direction.

Device	Spin speed (rpm)	AVT (%)	Scan direction	V _{oc} (V)	J _{sc} (mA/cm ²)	F.F (%)	η (%)	η _{avg} (%)	Deviation
PTAA	2500	6.3	Forward	1.1	19.3	74	15.7	15.8	14.45±0.76
			Reverse	1.1	19.3	75	15.9		
	3000	7.8	Forward	1.1	18.4	74	15.0	15.1	14.17±0.76
			Reverse	1.1	18.4	75	15.2		
	3500	9.6	Forward	1.1	17.8	74	14.4	14.5	13.58±0.69
			Reverse	1.1	17.9	75	14.6		
	4000	12.5	Forward	1.1	16.9	76	14.3	14.35	13.15±1.14
			Reverse	1.1	17.0	77	14.4		
	4500	15.3	Forward	1.1	15.8	75	13.2	13.25	12.14±0.99
			Reverse	1.1	15.8	76	13.3		
	5000	17.3	Forward	1.1	15.2	74	12.5	12.55	11.15±1.20
			Reverse	1.1	15.2	75	12.6		

750 nm-wavelength was gradually decreased from ~40 % (average visible transmittance (AVT) = 17.3 %) for 5000 rpm sample to ~18 % (AVT = 6.3 %) for 2500 rpm sample as shown in **Fig. 3(b)**. A photograph of full cell comprised with FTO/TiO₂/MAPbI₃/PTAA with additives/PEDOT:PSS/ITO, of which the MAPbI₃ film was deposited by spin-coating at 2500 rpm, shows its transparency as shown in **Fig. 3(c)**. The EQE (external quantum efficiency) spectrum in **Fig. 3(d)** did not show dip by absorption loss at ~650 nm-wavelength due to no absorption of PTAA. The photovoltaic properties of MAPbI₃/PTAA planar sandwich cell were shown in **Fig. 3(e)** and **Table 2**. The semi-transparent planar sandwich cell exhibited 1.1 V V_{oc}, 19.3 mA/cm² J_{sc}, 74 % F.F, and 15.7 % η for forward scan condition and 1.1 V V_{oc}, 19.3 mA/cm² J_{sc}, 75 % F.F, and 15.9 % η for reverse scan condition, thereby showing 15.8 % η_{avg} (see the detailed deviation of J_{sc}, V_{oc}, F.F and η_{avg} in **Fig. S4**) The J-V curve of back illumination was shown in **Fig. S2(b)** indicating that the average efficiency is decreased from 15.7 % to 13.8 %. The deviation of η_{avg} of 30 samples in **Fig. 3(f)** confirms reproducible fabrication of MAPbI₃/PTAA semi-transparent planar sandwich solar cells. To check the stability of MAPbI₃ planar sandwich solar cell, we measured η_{avg} and relative humidity in every day for 20 days as shown in **Fig. 3(g)**. The initial η_{avg} was 15.8 % and the η_{avg} after 20 days was 15.0 % so that ~5% of η_{avg} was degraded. This implies that the MAPbI₃ perovskite hybrid sandwich solar cells will have air and humidity stability if the cells are properly encapsulated. The current density variation with light soaking time under applied voltage at maximum power point was shown in **Fig. S5**. Here, the unsealed sandwich type solar cell was exposed by continuous 1 Sun light of solar simulator (100 mW/cm²) for 3600 s at air condition. During the continuous light illumination, the temperature of device was gradually increased to ~ 50 °C. Apparently the device efficiency is declining with light soaking time but currently it is not clear the efficiency is reducing by degradation or elevated temperature. Further studies should be required to check the photo- and thermal-stability of sandwich type perovskite solar cells under continuous light soaking condition.

Fig. 4 shows J-V curves of all MAPbI₃/PTAA planar sandwich solar cells with spin speed (rpm) under forward and reverse scan

direction. Their photovoltaic properties were summarized in **Table 2**. The J_{sc} of MAPbI₃/PTAA planar sandwich solar cell was gradually decreased with the spin speed because its transmittance is gradually decreased as well. Therefore, the η_{avg} was gradually decreased from 15.8 % to 12.55 %. This indicates that very efficient MAPbI₃ perovskite hybrid sandwich solar cells can be fabricated with transmittance of ~10 % to ~40 % at 700 nm-wavelength. Therefore, the semi-transparent MAPbI₃ planar sandwich solar cells might be applicable to BIPVs. It is noted that all MAPbI₃/PTAA sandwich cells did not show significant J-V hysteresis with respect to the scan direction as similar to the MAPbI₃/P3HT sandwich cells. This might be attributed to the reduced trap density of MAPbI₃ perovskite layer which is prepared with MAPbI₃/DMF solution with HI additive [6k] and the improved hole conductivity of HTMs due to the introduction of Li-TFSI and t-BP additives [5f] because the HI additives can prevent the formation of PbI₂ by decomposition of MAPbI₃ during the deposition process, thereby reducing the shallow trap density [6k] and the added Li-TFSI and t-BP in HTMs act as redox couple, thereby enhancing the regeneration of holes generated in MAPbI₃ perovskite [5f]. Therefore, the capacitance elements by traps in the MAPbI₃ sandwich solar cells are reduced, thereby shortening the delay time by trapping and de-trapping of charge carriers and the electron flux is fairly balanced with hole flux due to the improved hole conductivity even though the thickness of HTMs with additives are thick.

**Fig. 4.** J-V curves of full FTO/TiO₂/MAPbI₃/PTAA with additives/PEDOT:PSS/ITO planar sandwich solar cells with spin speed (rpm) measured under (a) forward scan and (b) reverse scan condition.

Conclusions

We could reproducibly fabricate semi-transparent MAPbI₃ perovskite planar sandwich solar cells by laminating FTO/TiO₂/MAPbI₃/wet HTM with additives and PEDOT:PSS/ITO. The FTO/TiO₂/MAPbI₃/P3HT with additives/PEDOT:PSS/ITO planar sandwich cell exhibited 12.8 % of η_{avg} without significant J-V hysteresis with respect to the forward and reverse scan direction and poor visible transmission due to strong absorption by P3HT. Whereas, the FTO/TiO₂/MAPbI₃/PTAA with additives/PEDOT:PSS/ITO planar sandwich cell exhibited 15.8 % of η_{avg} without significant J-V hysteresis with scan direction and good visible transparency. Moreover, the semi-transparent MAPbI₃ planar sandwich solar cells exhibited great air and humidity stability over 20 days so that we believe that the sandwich type perovskite hybrid solar cells can be applicable to BIPVs.

Acknowledgement

This study was supported by Mid-career Research Program (No.:NRF-2013R1A2A2A01067999), Basic Science Research Program (No. 2014R1A5A1009799), the Global Frontier R&D Program of the Center for Multiscale Energy System through the National Research Foundation of Korea (NRF) funded by the Ministry of Science, ICT & Future Planning, and the New & Renewable Energy Core Technology Program (No. 20133030000140) of the Korea Institute of Energy Technology Evaluation and Planning (KETEP) granted financial resource from the Ministry of Trade, Industry & Energy.

Notes and references

- 1 A. Kojima, K. Teshima, Y. Shirai, T. Miyasaka, *J. Am. Chem. Soc.* 2009, **131**, 6050.
- 2 S. D. Wolf, J. Holovsky, S.-J. Moon, P. Löper, B. Niesen, M. Ledinsky, F.-J. Haug, J.-H. Yum, C. Ballif, *J. Phys. Chem. Lett.* 2014, **5**, 1035.
- 3 V. D'Innocenzo, G. Grancini, M. J. P. Alcocer, A. R. S. Kandada, S. D. Stranks, M. M. Lee, G. Lanzani, H. J. Snaith, A. Petrozza, *Nat. Commun.* 2014, **5**, 3586.
- 4 a) G. Xing, N. Mathews, S. Sun, S. S. Lim, Y. M. Lam, M. Grätzel, S. Mhaisalkar, T. C. Sum, *Science* 2013, **342**, 344; b) S. D. Stranks, G. E. Eperon, G. Grancini, C. Menelaou, M. J. P. Alcocer, T. Leijtens, L. M. Herz, A. Petrozza, H. J. Snaith, *Science* 2013, **342**, 341.
- 5 a) H.-S. Kim, C. R. Lee, J. H. Im, K. B. Lee, T. Moehl, A. Marchioro, S. J. Moon, R. Humphry-Baker, J. H. Yum, J. E. Moser, M. Grätzel, N.-G. Park, *Sci. Rep.* 2012, **2**, 591; b) J. H. Heo, S. H. Im, J. H. Noh, T. N. Madal, C. S. Lim, J. A. Chang, Y. H. Lee, H.-J. Kim, A. Sarkar, Md. K. Nazeeruddin, M. Grätzel, S. I. Seok, *Nat. Photon.* 2013, **7**, 486; c) J. H. Noh, S. H. Im, J. H. Heo, T. N. Mandal, S. I. Seok, *Nano Lett.* 2013, **13**, 1764; d) J. H. Noh, N. J. Jeon, Y. C. Choi, Md. K. Nazeeruddin, M. Grätzel, S. I. Seok, *J. Mater. Chem. A* 2013, **1**, 11842; e) N. J. Jeon, J. Lee, J. H. Noh, M. K. Nazeeruddin, M. Grätzel, S. I. Seok, *J. Am. Chem. Soc.* 2013, **135**, 19087; f) J. H. Heo, S. H. Im, *Phys. Status Solidi RRL* 2014, **8**, 816; g) J. Burschka, N. Pellet, S. J. Moon, R. H. Baker, P. Gao, M. K. Nazeeruddin, M. Grätzel, *Nature* 2013, **499**, 316; h) N. J. Jeon, J. H. Noh, Y. C. Kim, W. S. Yang, S. Ryu, S. I. Seok, *Nat. Mater.* 2014, **13**, 897.
- 6 a) M. Liu, M. B. Johnston, H. J. Snaith, *Nature* 2013, **501**, 395; b) O. Malinkiewicz, A. Yella, Y. H. Lee, G. M. Espallargas, M. Grätzel, M. K. Nazeeruddin, H. J. Bolink, *Nat. Phot.* 2014, **8**, 128; c) D. Liu, T. L. Kelly, *Nat. Phot.* 2014, **8**, 133; d) J. H. Heo, D. H. Song, S. H. Im, *Adv. Mater.* 2014, **26**, 8179; e) Z. Xiao, Q. Dong, C. Bi, Y. Shao, Y. Yuan, J. Huang, *Adv. Mat.* 2014, **26**, 6503; f) J.-H. Im, I.-H. Jang, N. Pellet, M. Grätzel, N.-G. Park, *Nat. Nanotech.* 2014, **9**, 927; g) J. Seo, S. Park, Y. C. Kim, N. J. Jeon, J. H. Noh, S. C. Yoon, S. I. Seok, *Energy Environ. Sci.* 2014, **7**, 2642; h) M. Xiao, F. Huang, W. Huang, Y. Dkhissi, Y. Zhu, J. Etheridge, A. Gray-Weale, U. Bach, Y.-B. Cheng, L. Spiccia, *Angew. Chem. Int. Ed.* 2014, **126**, 10056; i) H. Zhou, Q. Chen, G. Li, S. Luo, T. -Z. Song, H. -S. Duan, Z. Hong, J. You, Y. Liu, Y. Yang, *Science* 2014, **345**, 542; j) J. H. Heo, H. J. Han, D. Kim, T. K. Ahn, S. H. Im, *Energy Environ. Sci.* 2015, **8**, 1602; k) J. H. Heo, D. H. Song, H. J. Han, S. Y. Kim, J. H. Kim, D. Kim, H. W. Shin, T. K. Ahn, C. Wolf, T. -W. Lee, S. H. Im, *Adv. Mater.* DOI:10.1002/adma.201500048.
- 7 a) M. M. Lee, J. Teuscher, T. Miyasaka, T. N. Murakami, H. J. Snaith, *Science* 2012, **338**, 643; b) J. M. Ball, M. M. Lee, A. Hey, H. J. Snaith, *Energy Environ. Sci.* 2013, **6**, 1739; c) D. Bi, S.-J. Moon, L. Häggman, G. Boschloo, L. Yang, E. M. J. Johansson, Md. K. Nazeeruddin, M. Grätzel, *RSC Adv.* 2013, **3**, 18762.
- 8 N. J. Jeon, J. H. Noh, W. S. Yang, Y. C. Kim, S. Ryu, J. Seo, S. I. Seok, *Nature* 2015, **517**, 476.
- 9 a) H. J. Snaith, A. Abate, J. M. Ball, G. E. Eperon, T. Leijtens, N. K. Noel, S. D. Stranks, J. T.-W. Wang, K. Wojciechowski, W. Zhang, *J. Phys. Chem. Lett.* 2014, **5**, 1511; b) H.-S. Kim, N.-G. Park, *J. Phys. Chem. Lett.* 2014, **5**, 2927; c) E. L. Unger, E. T. Hoke, C. D. Ballie, W. H. Nguyen, A. R. Bowring, T. Heumüller, M. G. Christoforo, M. D. McGehee, *Energy Environ. Sci.* 2014, **7**, 3690.
- 10 J. Yang, B. D. Siempelkamp, D. Liu, T. L. Kelly, *ACS Nano*, DOI: 10.1021/nn506864k (2015).
- 11 H.-S. Kim, I. Mora-Sero, V. Gonzalez-Pedro, F. Fabregat-Santiago, E. J. Juarez-Perez, N.-G. Park, J. Bisquert, *Nature Comm.* 2013, **4**, 2242.
- 12 J. M. Frost, K. T. Butler, F. Brivio, C. H. Hendon, M. van Schilfgaarde, A. Walsh, *Nano Lett.* 2014, **14**, 2584.
- 13 G. E. Eperon, V. M. Burlakov, A. Goriely, H. J. Snaith, *ACS Nano* 2014, **8**, 591.
- 14 L. K. Ono, S. Wang, Y. Kato, S. R. Raga, Y. Qi, *Energy Environ. Sci.* 2014, **7**, 3989.
- 15 C. Roldán-Carmona, O. Malinkiewicz, R. Betancur, G. Longo, C. Mombona, F. Jaramillo, L. Camacho, H. J. Bolink, *Energy Environ. Sci.* 2014, **7**, 2968.
- 16 Z. Li, S. A. Kulkarni, P. P. Boix, E. Shi, A. Cao, K. Fu, S. K. Batibyal, J. Zhang, Q. Xiong, L. H. Wong, N. Mathews, S. G. Mhaisalkar, *ACS Nano* 2014, **8**, 6797.
- 17 F. Guo, H. Azimi, Y. Hou, T. Przybilla, M. Hu, C. Bronnbauer, S. Langner, E. Spiecker, K. Forberich, C. J. Brabec, *Nanoscale* 2015, **7**, 1642.
- 18 W. Zhang, J. Smith, R. Hamilton, M. Heeney, J. Kirkpatrick, K. Song, S. E. Watkins, T. Anthopoulos, I. McCulloch, *J. Am. Chem. Soc.* 2009, **131**, 10814.

Broader context

The sandwich type semi-transparent planar perovskite thin-film solar cells using transparent top and bottom electrode like the dye sensitized solar cells are of great interest because they have self-passivated device architecture by two transparent electrode and good transparency, thereby readily applicable to the building integrated photovoltaics (BIPVs). Here, we demonstrated stable 15.8% semi-transparent $\text{CH}_3\text{NH}_3\text{PbI}_3$ (MAPbI₃) planar sandwich solar cells by simply laminating an FTO (F doped tin oxide) substrate/TiO₂/MAPbI₃/wet hole transporting material (HTM) with additives and a PEDOT:PSS (poly(3,4-ethylenedioxythiophene): poly(styrenesulfonic acid))/indium tin oxide (ITO) substrate. The average visible transmittance (AVT) was controllable from 17.3 % to 6.3 % by the thickness control of the MAPbI₃ layer.